Non-linear processes on Pt, Rh, Pd, Ir and Ru surfaces during the NO–hydrogen reactions

P.D. Cobden [a], C.A. de Wolf [a], M.Yu. Smirnov [b], A. Makeev [c], B.E. Nieuwenhuys [a,*]

[a] *Leiden University, Leiden Institute of Chemistry, Gorlaeus Laboratories, Leiden University, P.O. Box 9502, 2300 RA Leiden, Netherlands*
[b] *Boreskov Institute of Catalysis, SB RAS, 630090 Novosibirsk, Russia*
[c] *Department of Comput. and Cybernetics, Moscow State University, Moscow 119899, Russia*

Abstract

The present paper reviews our research in the field of $NO + H_2$ reactions over Pt, Rh, Pd, Ir and Ru surfaces. Emphasis will be placed on the ability of these platinum group metals to produce oscillations in both reaction rate and selectivity, in addition to other non-linear processes such as hysteresis phenomena. In the case of Rh, non-linearity is related to periodic transitions between N- and O-rich surfaces, with O destabilising the N-adlayer and causing an acceleration in the N_2 production. However, in the case of Pt, the important step involves the creation of vacant sites required for NO dissociation, whereby products leaving the surface facilitate an autocatalytic rise in the concentration of such vacancies and, hence, reaction rate. Ir positions itself between the former two, because oscillations have been observed in two different regimes. Both a lower-temperature Pt-like and higher-temperature Rh-like behaviours have been observed on different Ir surfaces. New results gained from field emission microscopy (FEM) and field ion microscopy (FIM) measurements are presented to consolidate the lower-temperature Pt-like behaviour, and confirm the dualistic nature of Ir. No oscillations in rate have been observed over Pd(111) or Ru(0001). The Ru surface exhibits selectivity to N_2 of almost 100% even in large excess of hydrogen. © 2000 Elsevier Science B.V. All rights reserved.

Keywords: $NO + H_2$ reactions; Oscillation; Non-linearity

1. Introduction

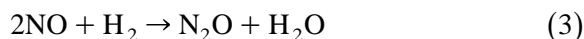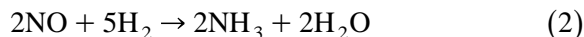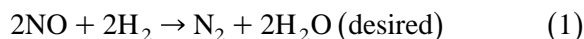### 1.1. NO reduction, non-linear behaviour

The recent interest in the reactions of NO with hydrogen has been greatly stimulated by the relevance of these reactions in automotive pollution control. The so-called three-way catalyst is capable of controlling CO, hydrocarbons and NO_x emission simultaneously using a single catalyst. This catalyst is based on Pt and Rh or Pd. The nitrogen oxides are converted into dinitrogen via reduction by hydrogen, hydrocarbons and CO. Unfortunately, dinitrogen is just one of a variety of reaction products that can be formed in the catalytic converters used in automobiles, due to the presence of various gases in the exhaust gas. Two of the undesirable reaction
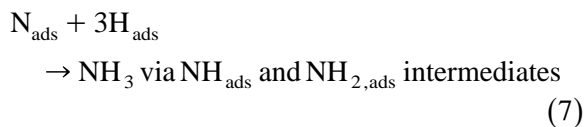
* Corresponding author. Tel.: +31-71-5274545; fax: +31-71-5274451.
  E-mail address: b.nieuwe@chem.leidenuniv.nl (B.E. Nieuwenhuys).

products are N_2O and NH_3. NO and H_2 can react via the following overall reactions:

$$2NO + 2H_2 \rightarrow N_2 + 2H_2O \text{ (desired)} \tag{1}$$

$$2NO + 5H_2 \rightarrow 2NH_3 + 2H_2O \tag{2}$$

$$2NO + H_2 \rightarrow N_2O + H_2O \tag{3}$$

In collaboration with the group of K.Tanaka, we have studied in detail the $NO + H_2$ reactions on a number of Pt, Rh and Pt–Rh alloy surfaces [1–3]. In particular, the mechanisms of the various processes resulting in the production of N_2, N_2O and NH_3 were investigated. It was concluded that the three N-containing reaction products N_2, NH_3 and N_2O are formed as follows:

$$NO_{ads} \rightarrow N_{ads} + O_{ads} \tag{4}$$

$$2N_{ads} \rightarrow N_2 \tag{5}$$

$$NO_{ads} + N_{ads} \rightarrow N_2O \tag{6}$$

$$N_{ads} + 3H_{ads}$$
$$\rightarrow NH_3 \text{ via } NH_{ads} \text{ and } NH_{2,ads} \text{ intermediates} \tag{7}$$

The availability of a vacant site near the NO_{ads} and N_{ads} may play a central role in the selectivity towards N_2O and N_2. A situation such as the one sketched as (b) below, where $\square$ denotes a vacant site on the surface, may result in additional NO bond breaking and in N_2 formation, whereas situation (a) will result in N_2O formation:

$$O\ O\ O \tag{a}$$
$$\underline{N\ N\ N\ N}$$

$$O$$
$$\underline{\square\ N\ N} \tag{b}$$

Both the activity and the selectivity are strongly dependent on structure and composition of the surface. Rh(100) is very selective to N_2 formation due to the presence of strongly bound N adatoms. On Pt(100), on the other hand, the Pt−N bond strength is much weaker resulting in a much lower concentration of N-adatoms and a poor selectivity to N_2.

Non-linear behaviour of surface reactions, including oscillations in rate and spatiotemporal pattern formation on the catalyst surface has become an active field of research in the past decade [4–6]. In general, the presence of strongly non-equilibrium conditions during chemical reactions can result in a variety of interesting effects such as oscillations, chemical waves, kinetic phase transitions, bistability, instabilities and chaos. All of these effects being mathematically due to the strong non-linearities in the kinetic rate equations describing these chemical processes [7].

The purpose of this article is to review our work on the oscillatory behaviour of NO reduction over metal surfaces. The choice of examples presented in this paper is driven primarily by our own research interests, and, therefore, does not represent the total body of relevant literature. Our ongoing research is concerned with two main questions: (1) Why can a heterogeneous catalytic reaction exhibit oscillatory behaviour under certain conditions? (2) How can such non-linear phenomena be used to broaden the mechanistic understanding of reactions? The investigation of reactions under such dynamic situations will lead to a better understanding of reactivity and mechanism in less obvious non-linear situations. The mechanisms that cause non-linear behaviour are almost always present, and so in studying cases where they are predominant, the breadth of knowledge of these reactions can be refined.

It is realized now that there is no universal mechanism. For the sake of convenience, models for oscillations in surface reactions can be divided into two main categories: (i) non-isothermal models and (ii) isothermal models.

(i) The non-isothermal model. This model is one of the major mechanisms for oscillations of exothermic reactions over supported metal catalysts in the higher-pressure range. The heat released by the reaction cannot be transported sufficiently via the non-conducting support.

(ii) The isothermal model. This general model can be subdivided into a number of classes,

which have in common a periodic transition between two surface states with different activities: (a) transitions between two states, differing in chemical composition. Examples include transitions between an oxidized and reduced metal surface and transitions between an almost adsorbate-free and adsorbate covered surface with the reaction being inhibited on the latter. b) Adsorbate-driven transitions between two surface structures with different activities. The oscillatory processes discussed in the present paper belong to category (ii).

2. Non-linear behaviour in the catalytic reduction of NO

The reaction dynamics of the $NO + H_2$ system over several noble metal surfaces has been studied on the microscopic [8–11], mesoscopic [12,13] and macroscopic scales [4,5,14–17], using field electron microscopy (FEM, resolution 15 Å), photoemission electron microscopy (PEEM) and macroscopic rate measurements, respectively. PEEM is the most widely used technique for imaging spatiotemporal processes on surfaces. PEEM only allows the investigation of surfaces with spatial resolution on the mesoscopic scale (1 μm). The introduction of FEM and FIM for following the progress of oscillatory processes increased the spatial resolution to the microscopic scale (~ 15 Å).

2.1. The microscopic scale

The first FEM study used to analyse an oscillatory process on a microscopic scale was the reduction of NO with H_2 over an Rh field emitter [8]. Sustained oscillations were observed around 460 K. These oscillations took the form of a regular variation of the emission current as a result of moving waves that spread across the majority of the field emitter tip. They started at the (533) and (321) planes and possibly the edges of the (111) plane and travelling around the tip parallel to step edges [4,8,9]. However,

not all of the crystal planes present on the tip took part in the variation of the emission current, notably the (100) and (210) planes [8,9].

Fig. 1 shows as an example the behaviour of the Rh(533) interface surface. Surface defects and grain boundaries were also seen to have an influence on the initiation of the surface waves [9]. At the lower temperature of 430 K, the four quadrants of the [100]-oriented tip are observed to act independently of each other. Here, the wave does not spread over the whole surface; it still begins at the (533) plane, but is unable to traverse the (320) plane, as was the case at higher temperatures. The effect of decreasing the H_2 pressure is similar, in that it can also decrease the ability of the wave to cross over the (320) area. On increasing the H_2 pressure, the temperature at which oscillations occurred decreased.

Local independent oscillation centres have also been observed for the reaction on Ir field emitters in the 10^{-7} to 10^{-6} mbar range and temperatures between 330 and 370 K [11]. Sustained isothermal oscillations were observed on a number of surfaces near (100). The oscilla-
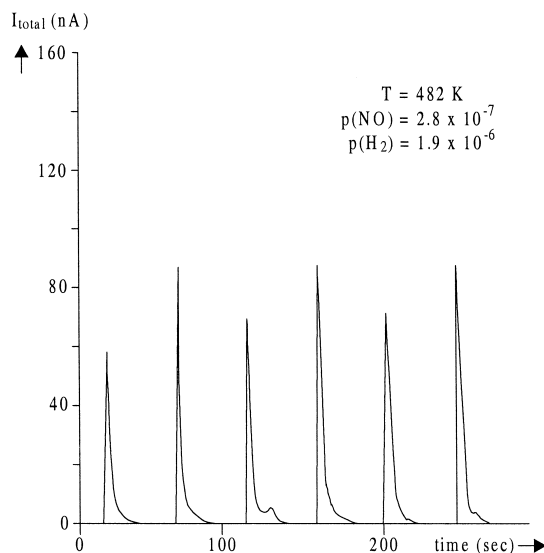

Fig. 1. The variation of the emission current from the Rh (533) plane as a function of time during the oscillatory behaviour of the $NO + H_2$ reaction on an Rh field emitter, $T = 482$ K (from Ref. [8]).

tions were manifested by periodic changes in emission intensity. The three (100) areas of a [111]-oriented tip oscillated independently of one another. A very similar behaviour could be found over a [111]-oriented Pt tip, conditions where all three oscillation centres oscillated in phase with one another. The intensity variation took place on the stepped surface around the three Pt(100) planes, and not on the (100) planes themselves [4,10].

2.2. The mesoscopic scale

Mesoscopically, spatiotemporal behaviour in the NO + H_2 reaction has also been observed with PEEM on large Rh single crystal surfaces in the form of chemical waves travelling across the surfaces [12,13]. The shape of these waves depends on the structural changes that were induced by N and O on the surface. The O and N interaction with Rh surfaces has been discussed in detail by Comelli et al. [18]. In the PEEM study new species have been observed on Rh(111) characterized by a work-function drop below that of the clean surface when two or more reaction fronts collide [13]. This species has been attributed to a subsurface oxygen species [13], although a mathematical model developed for this system indicates that it could be a function of two highly reactive, low coverage areas colliding in a synergetic manner [19].

2.3. The macroscopic scale

On the macroscopic scale, the reaction has been studied over a number of selected large single-crystal surfaces of Rh, Pt, Ir, Pd and Ru using mass spectrometry [4,5,10,11,14–18,20, 22,23]. The selection of surfaces was partly based on our previous FEM studies, and a wide variety of non-linear behaviour was revealed. The reaction over Ir(110) and (210), Pt(100) and various (111)-terraced Rh planes showed sustained isothermal oscillations in product formation under certain experimental conditions (*T* range, H_2 and NO pressures). In all cases, N_2

and NH_3 were formed. For Rh [4] and Ir [16,17] the formation of these products occurred out of phase with each other, whereas for Pt, it occurred in phase [14]. The latter is illustrated in Fig. 2. For Pt, the of out-of-phase formation of N_2O is also a strong indicator of the vacancy description for N_2 and N_2O formation suggested earlier in this text. In the case of Ir(100) damped oscillations were seen on cooling, with N_2 and H_2O being produced in phase, and no associated NH_3 formation. There is, however, an indication of the formation of an NH_x species present on the surface [11].

The Rh surfaces on which oscillatory behaviour was observed have in common that they consist of (111) structures. The same structure sensitivity was observed as in our FEM studies. For example, the stepped Rh(533) shows oscillatory behaviour whereas Rh(100) is not active under similar conditions. By changing the step density on the (111) like surfaces, information was obtained about the effect of terrace width on the oscillatory behaviour. The NO + H_2 reaction is rather similar over Rh(533), Rh(311) and Rh(111) [4].

Fig. 3 shows recent results of the oscillatory behaviour observed over Ir(110). Clearly, the selectivity towards N_2 and NH_3 oscillates: the rate of N_2 formation ($r(N_2)$) is exactly out of phase with the rates of formation of NH_3 and
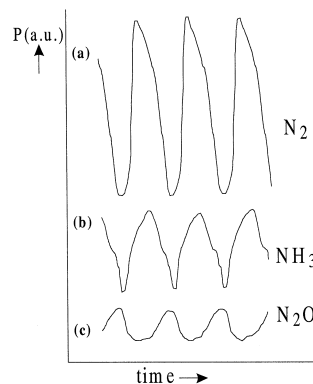

Fig. 2. Variations of the N_2, NH_3 and N_2O partial pressures during the NO + H_2 reaction over Pt(100) as a function of time. $T = 460$ K, $p(NO)$ and $p(H_2) = 3 \times 10^{-6}$ mbar (adopted from Ref. [14]).
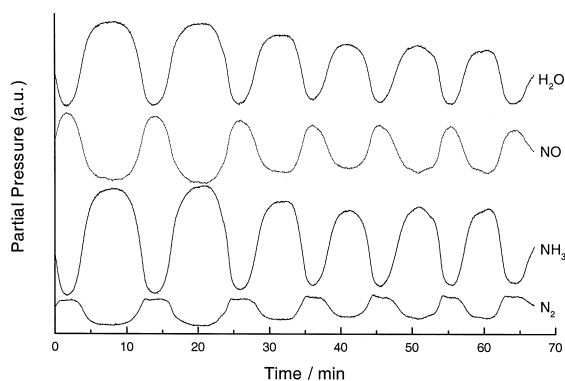
Fig. 3. Oscillatory behaviour in the $NO + H_2$ reaction rate over Ir(110) at 479 K with $p(NO) = 7.7 \times 10^{-7}$ mbar and $H_2/NO = 20$. The partial pressures of H_2O, NO, NH_3 and N_2 as a function of time (from Ref. [16]).

H_2O ($r(NH_3)$ and $r(H_2O)$). No N_2O is formed. Hence, reaction (3) does not occur under the experimental conditions used. The NO signal is out of phase with the NH_3 and H_2O signals. This indicates that at a high consumption of NO, i.e., at a low NO signal in the gas phase, the H_2O and NH_3 formation rates are high. Therefore, a direct relation exists between the conversion of NO and the formation rates of H_2O and NH_3. Such a relation does not exist between $p(NO)$ and $r(N_2)$. In the oscillatory regime the NO and N_2 are clearly in phase. Apparently, the N_{ads} atoms formed from the decomposition of NO have to compete with the O_{ads} in the reaction with H_{ads} atoms to leave the surface as NH_3 and H_2O, respectively. Since H_2O is more easily formed, part of the N_{ads} remains on the surface before it can react to form gaseous N_2

The rate oscillations are obtained by variation of the hydrogen pressure while keeping the temperature constant in the temperature range where the selectivity changes from N_2 to NH_3 or vice versa. Over Rh, the rate oscillations are obtained by heating or cooling the surface in the reactant mixture until a transient region is reached. This region is coupled to a hysteresis in the formation rates of N_2 and NH_3, as Fig. 4 illustrates for the $NO + H_2$ reaction over

Rh(533). Fig. 4 indicates that $r(NH_3)$ and $r(N_2)$ are competitive processes, in particular in the transient region. That is, both $r(N_2)$ and $r(NH_3)$ are again out of phase.

During a heat and cool cycle under comparable conditions, the $NO + H_2$ reaction over Ru(0001) looks very different [20]. As shown in Fig. 5, a large hysteresis is observed in the formation rates of N_2 and H_2O, but hardly any NH_3 is formed. Another difference with the Rh and Ir surfaces is the absence of low temperature N_2 formation. Obviously, over Ru(0001) there is no competition between the formation of N_2 and NH_3.

Using in situ AES a high coverage O-layer was observed on the heating branch, while no N-species were present on the surface when N_2 was formed. Since NH_3 (or N_2O) is not formed, this means that the NO dissociation and the reaction between N_{ads} and N_{ads} proceed very fast. The O-layer could not be completely removed by the reaction with hydrogen even at temperatures higher than 800 K, indicating that the removal of O_{ads} by H_{ads} is the slow step which determines the minimum temperature required for full NO conversion. This was also observed for the $NO + H_2$ reaction over supported Ru catalysts [21]. Upon cooling the surface in the reaction mixture the lifetime of the
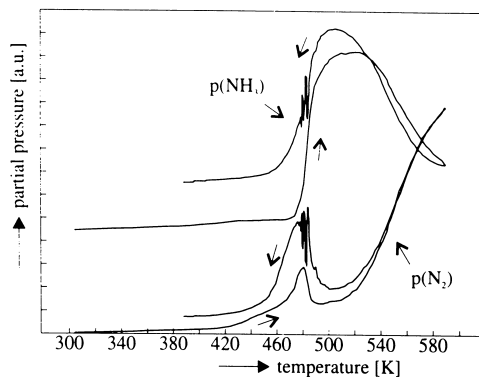

Fig. 4. $NO + H_2$/Rh(533), the rate of N_2 and NH_3 formation as a function of temperature at $p(NO) = 0.8 \times 10^{-6}$ mbar and $H_2/NO = 15$, the heating and cooling rate is 0.10 K s^{-1} (from Ref. [4]).

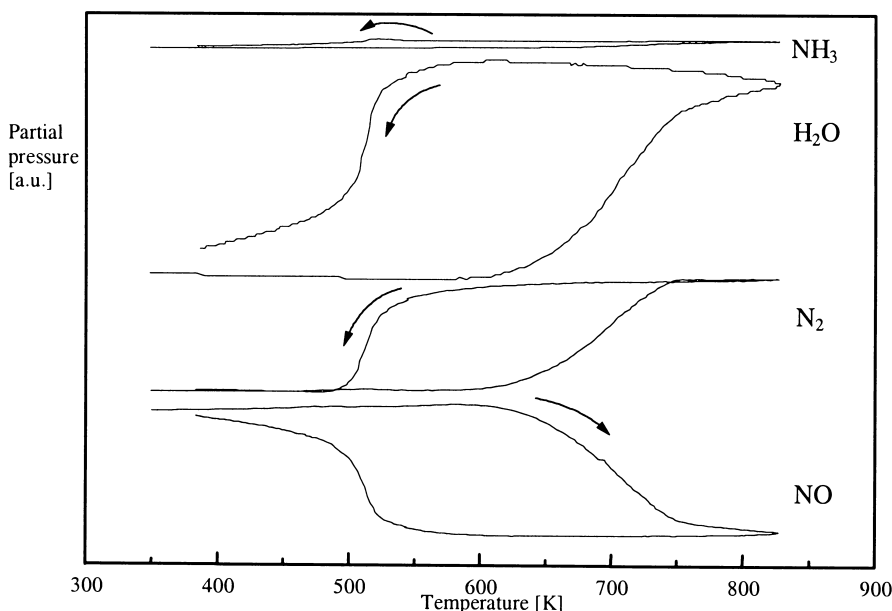Fig. 5. $NO + H_2/Ru(0001)$, the rate of NH_3, H_2O and N_2 formation and the conversion of NO as a function of temperature at $p(NO) = 7.8 \times 10^{-7}$ mbar and $H_2/NO = 20$, the heating and cooling rate is 0.5 K s^{-1} (from Ref. [20]).

H_{ads} increases allowing the reaction between O_{ads} and H_{ads} to proceed and all the O_{ads} reacts to form gaseous H_2O. At 500 K, the overall reaction (1) is stopped. This temperature is independent upon the hydrogen pressure. By comparing these results with the results of the $O_2 + H_2$ reaction over Ru(0001) [20], it appeared that under these conditions no reaction between H_{ads} and O_{ads} takes place below 500 K leading to an O-covered surface which blocks further reaction. At present, no oscillations were observed for the $NO + H_2$ reaction over Ru(0001).

The $NO + H_2$ reaction over Pd(111) was also examined. Apart from N_2 formation, large amounts of NH_3 and some N_2O were formed over this surface. However, non-linear behaviour was not observed during a heat and cool cycle.

Monitoring of the reaction products in the gas phase provides useful, but insufficient information to reveal the mechanism of the oscillatory behaviour, because knowledge about the chemical nature and concentrations of the species on the surface is lacking. In situ chemical analysis of the species present on the surface

during an oscillation cycle is required. Until now, the number of studies in which surface species have been directly monitored under non-linear reaction conditions is very scarce. In principle the recently developed technique of fast X-ray photoelectron spectroscopy (XPS) has the ability to monitor surface species in real time. High-resolution XPS spectra can be collected within 10–20 s using the super ESCA beamline at Elettra, the third generation synchrotron radiation source in Trieste.

Our recent studies [22–25] have shown that the high time and energy resolution of this technique allows for the determination of the changes occurring in the adsorbate layer during the hysteresis and for the identification of transient species which would be very difficult to trace using conventional widespread technology. On Rh(533) three nitrogen species, molecularly adsorbed NO, adsorbed N atoms and a third N species, which might be attributed to NH_x were detected during the $NO + H_2$ reaction [22–24]. Very recently, similar experiments revealed NO_{ads}, O_{ads} and probably only one N_{ads} species on Ir(110) during the hysteresis [25].

Fig. 6 shows for Rh(533) the variations of the coverages of NO_{ads}, N_{ads} and O_{ads} as identified and evaluated from the fitted O_{1s} and N_{1s} spectra during a heating and a cooling run for an $NO:H_2$ ratio of 1:5. In the same figure, the changes in the reaction rate manifested by the mass-spectrometer N_2 signal are displayed as well.

It is evident from Fig. 6 that both the surface species' coverages and the reaction rate show bistability: there are two surface states of differing composition and reactivity. On heating up the reactivity remains very low up to 520 K; the surface is essentially covered with atomic O and there is only a very small amount of atomic nitrogen. On the cooling branch, on the other hand, the surface is reactive until 480 K, with essentially very little oxygen on the surface, but a sizeable amount of N. Since there is no molecular NO on the surface > 450 K, NO_{ads} does not play a role in the hysteresis.

Let us follow one heat and cool cycle, starting with the heating branch. Initially, the atomic oxygen signal (Fig. 6) shows an increase up to ca. 470 K, whereas the N signal slightly increases before dropping again > 430 K. At the same time the molecular NO signal decreases, the N_2 production is low, and the H_2O production at this point in the hysteresis remains below the detection limit. The increase in the O and N signal is slower than the decrease of the NO signal, suggesting partial NO desorption. This
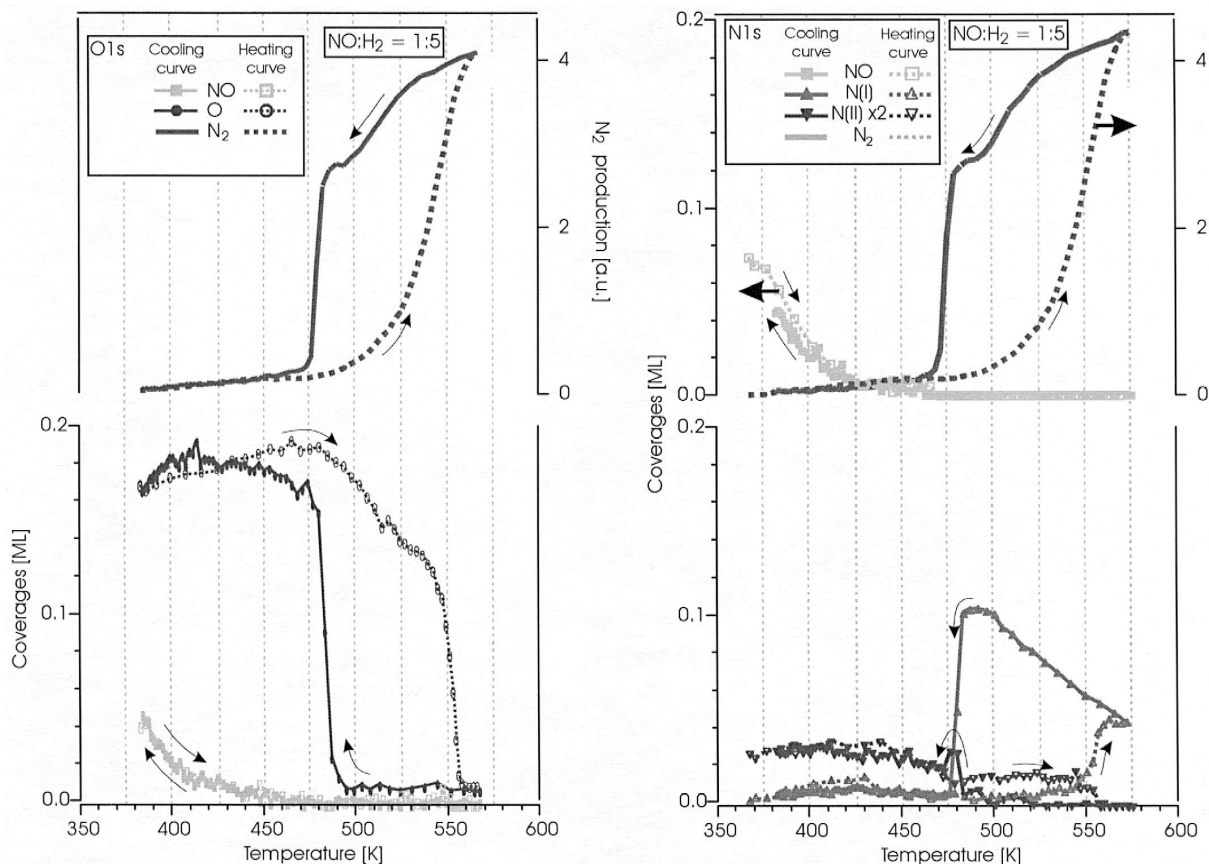

Fig. 6. Hysteresis in the coverages of atomic oxygen and nitrogen as well as in the production of N_2 upon cycling the temperature in the NO + H_2 reaction over Rh(533) in a flow of $p(NO) = 3 \times 10^{-7}$ mbar and $H_2/NO = 5$. The dashed lines/open symbols represent the heating branch, the solid/filled symbols the cooling branch (from Refs. [22,23]).

desorption opens space for the remaining NO molecules to dissociate into atomic N and O, while preventing H_2 from gaining access to the surface. The drop of the N signal > 430 K is due to nitrogen desorption by destabilization via repulsive interactions arising in the coadsorbed $O + N$ adlayer. The fact that there is no H_2O production at this point indicates that H_2, unlike NO, has no access to the surface. This argument is strengthened if the high reactivity of coadsorbed O and H is considered. Above 470 K, the O coverage starts to drop, reaching half of its maximum value by 550 K, whereas the stationary coverage of atomic N remains low. The N_2 production starts to increase continuously as the amount of oxygen on the surface decreases. This N_2 stems from recombination of N_{ads} (path 5).

The data indicate that up to ca. 550 K, when the O signal rapidly drops to a coverage of ca. 0.01 ML, the H_2 access to the surface remains partially suppressed. Once the oxygen coverage is strongly reduced, the H_2 is able to remove almost all atomic oxygen coming from NO dissociation. At this high temperature, when the reaction becomes very fast, the N coverage grows reaching significant amounts.

On the cooling branch, starting from high temperatures, N_{ads} continuously increases until 495 K and then remains constant until 480 K. The rate of N_2 production is decreasing but high enough to prevent the accumulation of nitrogen coverages, which could block the reaction. The H_2 adsorption seems not to be suppressed by the N coverage and keeps the rate of H_2O production high as well as the oxygen coverage very low. The N_2 production levels off around 490 K and drops rapidly afterwards. At the same time, the N coverage decreases dramatically, whereas the amount of oxygen on the surface increases rapidly. This switching can be explained as follows: by decreasing the temperature, the nitrogen coverage exceeds a critical value above which the dissociative H_2 adsorption is blocked, resulting in an incomplete oxygen removal. Oxygen accumulates (already

before the N_2 production levels off, see Fig. 6) and blocks severely further H_2 adsorption. Below 450 K, the surface is completely deactivated by the oxygen adlayer and only molecular NO can still adsorb. The oxygen layer destabilizes the N_{ads} species and accelerates its desorption. This is consistent with the fact that the drop in the N coverage precedes that of the N_2 production.

On Ir(110), an oscillatory behaviour was found under hydrogen rich conditions. The period and shape of the oscillations are rather different compared to Rh. However, recent fast XPS measurements suggest that the mechanism is rather similar to that discussed for Rh(533) [25].

At low H_2–NO ratios, the hysteresis in the integrated N_{ads} and O_{ads} XPS signal are comparable to Fig. 6, except for the increase in the N_{ads} at higher temperatures on the heating branch, which is not observed over Ir(110). At higher ratios where NH_3 formation starts to play a role, a build-up of an N-species is observed during the NH_3 formation. Tentatively, this N-species is attributed to N_{ads}, but a more careful evaluation of the results is necessary. On the cooling branch, as dissociative hydrogen adsorption is suppressed, O_{ads} no longer reacts to gaseous H_2O and a build-up of O_{ads} is observed leading to an immediate removal of N_{ads} by reaction (5), which suggests a repulsive interaction between N_{ads} and O_{ads}.

On the basis of these and other findings the following mechanism for the oscillatory process on Rh and certain Ir surfaces can be suggested.

1. During NH_3 formation, part of the N accumulates on the surface until this results in suppression of H_2 adsorption.
2. Because of the reduced amount of H on the surface, O atoms begin to accumulate. Repulsive O–N interactions enhance the rate of N_2 formation.
3. The fast removal of N results in a large depletion of the amount of atomic nitrogen on the surface. As a consequence, the rates

of NO and H_2 dissociative adsorption increase.

4. O is quickly removed by hydrogen. N atoms start to accumulate again on the surface: the cycle is repeated.

On Pt(100) sustained oscillations in rate and selectivity have been observed in a much wider range of temperatures and NO/H_2 ratios than on Rh and Ir surfaces. Small changes in the reactant ratio lead to a series of period doublings resulting, finally, to a state of deterministic chaos or aperiodic behaviour [14]. The molecularly adsorbed NO plays a key role in the mechanism of the oscillations on the Pt(100) surface, whereas on Rh surfaces and some Ir surfaces, it is only the supplier of N_{ads} and O_{ads}. A dispute in the literature concerns the role of the adsorbate induced $(1 \times 1) \leftrightarrow$ hex surface phase transition of Pt(100) in the mechanism of oscillatory behaviour of catalytic reactions on this surface. Cobden et al. [14] described the oscillations in terms of a vacancy model. In the low reactivity state the surface is blocked by NO_{ads}. Vacant sites are needed for NO dissociation and reaction. The important step in this mechanism involves the autocatalytic creation of vacant sites required for NO dissociation and, hence, for reaction. However, according to Walker et al. [26] and Gruyters et al. [27], the driving force for the oscillations is the combination of the hex phase $\leftrightarrow (1 \times 1)$ phase transition, the non-linear growth of (1×1) island growth from the hex phase and the low reactivity of the hex phase. Our recent simulations show that the phase transition is not essential for producing oscillatory behaviour [28,29]. The strongly non-linear dependence of NO_{ads} dissociation on the number of vacant Pt sites is the important factor. The surface phase transition results in a wider range of temperatures, where oscillations take place.

2.4. The dualistic nature of Ir

Ir appears to be a special case because two different mechanisms have been proposed for oscillations in two distinct regimes. A possible mechanism for the oscillations on the Ir(100) surface (and Ir tips) is one where NO_{ads} (and/or possibly O_{ads}) cause a decrease in the desorption energy of NO. Here, the desorption of NO from an NO_{ads} covered surface leads to an autocatalytic clearing of the surface (similar to that proposed to the Pt(100) surface [4,14]). The resulting surface is open for adsorption and rapid reaction of NO and H_2. The absence of NH_3 formation in the gas phase for the same reaction over Ir(100) in the relevant low temperature range points to the role of NH_x as a buffer species in the oscillating reaction [30]. The NH_x builds up on the surface (because it does not leave as NH_3), and slows the reaction. A slow replacement of NH_x by NO then occurs to complete the cycle. At these temperatures, EELS result show that NO can still be present on the surface [31], and this would suggest a vacancy mechanism similar to that suggested for this reaction over Pt(100) [4,14].

In FIM, the $NO + H_2$ reaction over Ir shows continuous pattern formation and destruction on the (100) and surrounding planes in the same parameter range as used in the field emission mode. This has been observed for both orientations of the tip. In the FIM mode, the lower limit for the $NO:H_2$ ratio decreases to 1:10. Fig. 7 represents such reactivity for a [100]-oriented tip. There is initially the growth of a grey area around the (100) plane (Fig. 7a–c), which has slightly brighter edges. In this case, after 7.0 s, there is an increase in emission from within this grey area, which within 1 s, rapidly expands as a ring reaching the rim of this area (Fig. 7d–g). The new grey area that remains starts to fade, beginning with (100) surfaces with (111) steps (Fig. 7g–j). Fig. 7k–l shows clearly the cross form, which breaks up into distinct bright spots, which also fade. The next build up phase begins, as shown in Fig. 7m, in two separate areas. The grey area around the (100)-plane shows stable growth until 24 s, when the bright wave is once again initiated. It should be noted that the time scale for this process is a order of
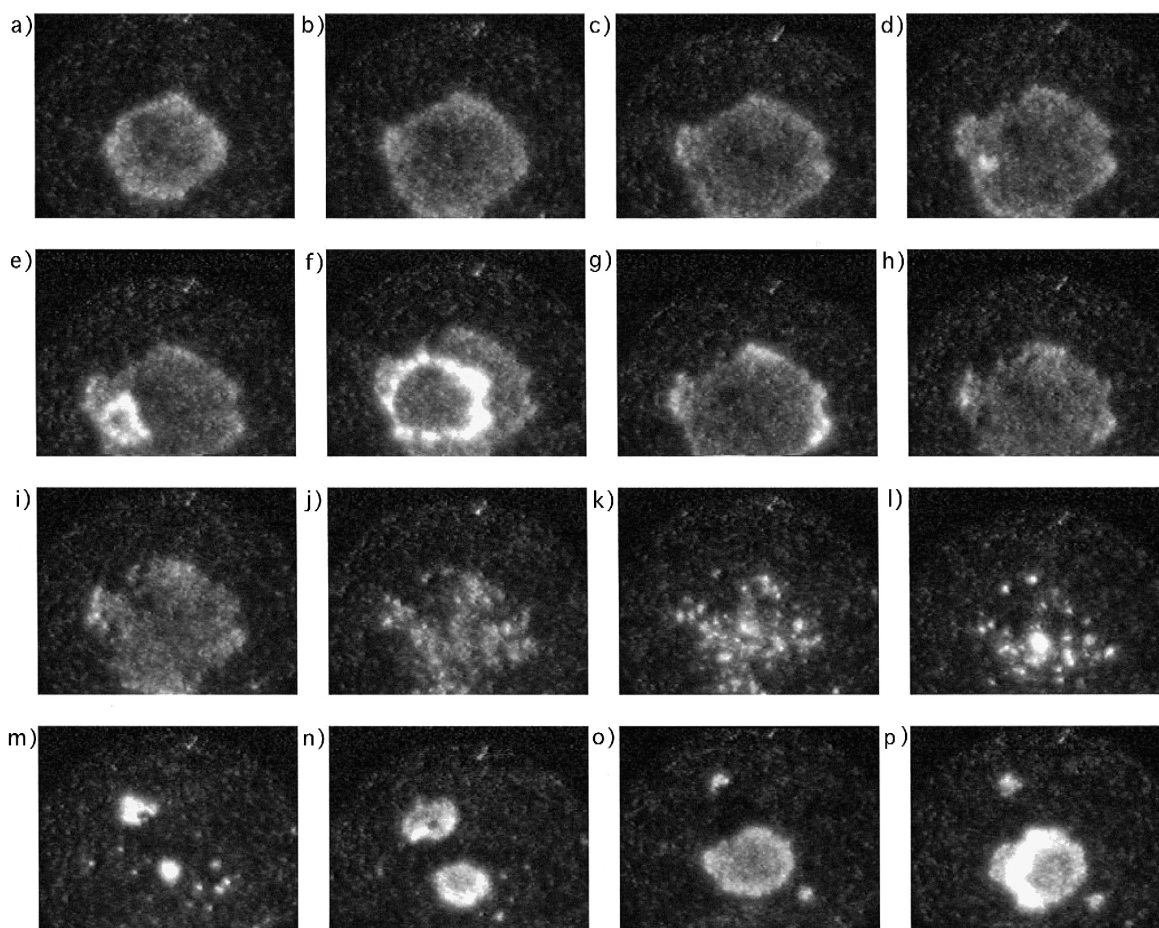
Fig. 7. Pattern formation in the NO + H_2 reaction, imaged with FIM at 349 K, $p(NO) = 2.4 \times 10^{-6}$ mbar and $p(H_2) = 6.25 \times 10^{-5}$ mbar. Images recorded at (a) 0.0 s, (b) 2.0 s, (c) 5.0 s, (d) 7.0 s, (e) 7.3 s, (f) 7.6 s, (g) 8.0 s, (h) 8.3 s, (i) 8.5 s, (j) 9.5 s, (k) 10 s, (l) 11 s, (m) 13 s, (n) 17 s, (o) 22 s and (p) 24 s.

magnitude faster that for the oscillations observed in FEM under similar conditions. Also the extent to which the grey areas grow is not constant. Indeed on a [111]-oriented tip, sometimes, the different grey areas around the (100)-planes, expanded to the extent that they overlapped. In such a case, once the bright wave was initiated, it moved rapidly across the whole joint area. At higher temperatures (360–370 K), even if these areas were separated, once the wave initiated in one area, it would also initiate in the other areas. This was not the case at lower temperatures (330–360 K) where, as in the case of FEM, the wave would be initiated around the different (100)-planes independently.

The oscillatory cycle proposed above for the NO + H_2 reaction over Ir(100) is also consistent with the observed behaviour in FIM. No specific imaging gas was introduced, so this function must be performed by one of the reactants or products with a low ionisation potential or a large permanent dipole. In this case, the imaging gas is most probably NO, which has by far the lowest ionisation potential. Assuming the reaction cycle given above, the FIM images relate to the following situation. The build up of the grey phase represents an NO_{ads} or possibly mixed NO_{ads} and O_{ads} adlayer. The higher work function of this area leads to increased imaging compared to the dark areas on the tip. The

edges of this grey area are slightly brighter indicating that there is a reaction front here. When the bright wave begins, it is initiated from within the grey area. This is analogous to the beginning of the autocatalytic cleaning of the surface. The reason for this high intensity wave is that H_2 is gaining access to this ad-layer, and all O_{ads} formed from the dissociation of NO is quickly mopped up, with the H_2O that is formed being ionised as it leaves the surface. This stage in FIM is analogous to the rapid increase of intensity that occurs in FEM. The remaining grey area consists of mainly N_{ads}, which either reacts with itself to form N_2 or with H_{ads} to form NH_x. The remaining bright spots being areas not yet overwhelmed by NH_x. A tip covered with NH_x will most probably be dark in FIM, and the build up of an NO_{ads} layer is once again observed.

The issue of the time scale and regularity of the events in FEM and FIM should be addressed. In FIM, the high positive field on the tip increases the gas supply to it, this higher apparent pressure could then lead to an increase in speed of the oscillatory cycle. H_2O, which has one of the largest permanent dipoles of simple molecules, is more strongly influenced by this phenomenon. In order to resolve the problem of possible interference of H_2O with the FIM results, atom probe FIM would have to be used.

Until now, the evidence for NH_x has been rather anecdotal. A relatively small amount of adsorbates on the tip together with the formation of NH_x would lead to a lower work function. The fact that the emission from the Ir(100) plane is much greater than that of the clean surface at the same voltage does indicated a work function reducing intermediate [11]. This is not necessarily true, because it is known for example that NO can change the morphology of Rh tips [32]. So, in addition to the dark FIM images, yet more evidence is needed to support this idea.

To this end, the $NO + NH_3$ reaction was also studied using FEM, with the underlying idea

that many of the mechanistic steps involved in this reaction would be similar to those in the $NO + H_2$ reaction. Similarities in reaction pathways between the $NO + H_2$ and $NO + NH_3$ reactions over Pt(100) have been used before to clarify the mechanism of oscillations [33]. Fig. 8 shows mainly several stages in the heating branch of a hysteresis in the $NO + NH_3$ reaction. The heating sequence (Fig. 8a–e) looks very similar to the $NO + H_2$ reaction [10]. The emission initially increases on step planes around the central (100) plane, in this case the (511) plane (Fig. 8b), and then spreads to the (100) plane itself (Fig. 8d). At higher temperatures, the increase in emission from the (100) plane reduces once again. Fig 8f shows the situation at room temperature, 500 s after a hysteresis cycle in a more NH_3 rich environment. It also helps to illustrate the fact the increase of emission on the central (100) plane is more stable during reaction with NH_3 than with H_2. Oscillations were not found for this particular reaction. This may have been because at RT, the increased emission on the (100) died away very slowly (typically greater than 3600 s), meaning if there are oscillations, they would have very long periods. The fact that the $NO + NH_3$ reaction gives very similar FEM images to the $NO + H_2$ reaction also gives a strong indication of the participation of NH_x (possibly also NH_3) in this step. The greater observed stability of the increased emission on and around the (100) areas also allude to the involvement of an NH_x species. Also, in the $NO + H_2$ case, an increase in H_2 pressure pushes the initiation of the increase in emission to lower temperatures, pointing to the involvement of hydrogen in the crucial changes that occur in surface adsorbate composition.

When comparing the $NO + H_2$ reaction on the Ir tip and the Ir(100) surface, it is important to take into account that the reaction on the Ir tip is initiated on the Ir(510) plane. This points in the direction of defects (more open surfaces) seeding the oscillations. In which case, diffusion of reactants from the (100) to the (510) area
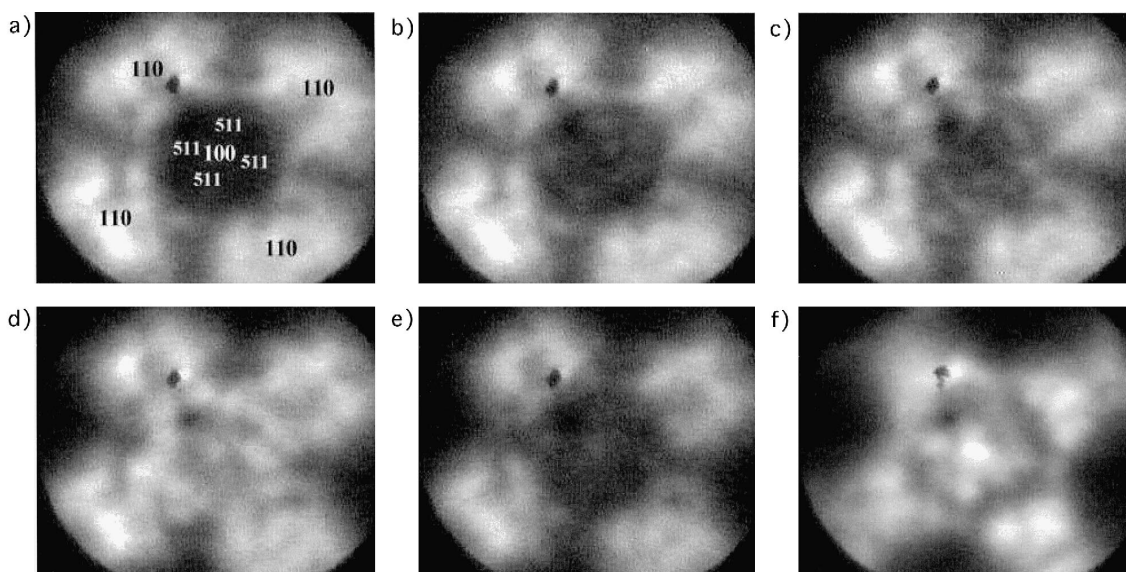
Fig. 8. FEM images observed during the NO + NH$_3$ reaction over Ir during heating branch of a hysteresis, with $p(NO) = 3.0 \times 10^{-6}$ mbar and $p(NH_3) = 1.0 \times 10^{-6}$ mbar and heating rate 0.8 K s^{-1}: (a) 305 K, (b) 340 K, (c) 355 K, (d) 400 K and (e) 440 K. (f) FEM image after 600 s at RT, after hysteresis cycle $p(NO) = 1.0 \times 10^{-6}$ mbar and $p(NH_3) = 1.0 \times 10^{-6}$ mbar.

also opens up the possibility of reaction on the (100) planes, which could explain why only damped oscillation are found on the extended Ir(100) surface.

The hysteresis seen on Ir(100) is also similar to the hysteresis for various Rh single crystal surfaces as also reported above. However, these phenomena occurred at lower temperatures, which would give reason to speculate that NO$_{ads}$

is more likely to play a role in the mechanism, than is the case for the Rh and certain other Ir surfaces, where N$_{ads}$ plays a more crucial role. In the case of Ir(110) the hysteresis seen in the NO + D$_2$ reaction was attributed to the presence of a saturated layer of oxygen and NO, which strongly inhibits the adsorption of D$_2$ [34]. Indeed, as described above, oscillations of a more Rh-like nature have also been found.
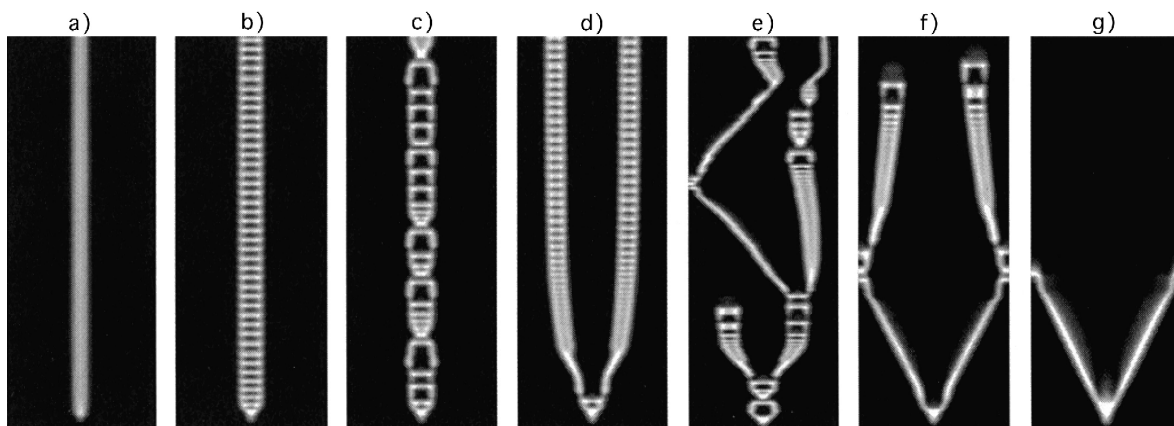

Fig. 9. Space–time plots (the time axis is vertical with initiation at the bottom) of the θ_{NH} values at $T = 456$ K and different values of $p(H_2)$: (a) 8×10^{-6}; (b) 9.4×10^{-6}; (c) 9.6×10^{-6}; (d) 9.7×10^{-6}; (e) 9.9×10^{-6}; (f) 1×10^{-5}; (g) 1.1×10^{-5} mbar (from Ref. [36]).

Mathematical modeling of the complex temporal (e.g., oscillatory) behaviour observed for the NO + H$_2$ reaction on Ir(110) based on the model described above for Rh(533) reproduces the experimental results [35]. A related model has been used for simulation of the complex phenomena described for Rh(111)/Rh(533) [36]. This space-independent model which includes the rate constants of the relevant elementary steps and the parameters of lateral interactions in the adlayer has been extended to a spatially distributed model by adding a mathematical description of the diffusion of the adsorbed particles over the surface [19]. This simulation reproduces the experimentally found spatial pattern formation: spiral waves and target patterns formed by spiral pairs are the dominant patterns both in the simulation and in the experiment. In addition, the model predicts a variety of self-organization phenomena that have not yet been found in the experiment. An example is shown in Fig. 9.

3. Conclusion

It is planned to extend our studies in this field by using various Group VIII metal surfaces and some selected alloy surfaces. It is anticipated that owing to further development of experimental methods and the increasing use of more advanced mathematical modeling our insights into the fascinating area of oscillatory surface reactions will increase in the next decade. New generations of STM could give information on variations in local surface structure during oscillations. There is an urgent need to analyze the species present on the surface during oscillations. Fast and non-destructive techniques are now available for this purpose. Our ultimate purpose is to obtain sufficient data that will enable to calculate under what conditions and with which mechanism a reaction oscillates on the different Group VIII metal surfaces.

References

[1] J. Siera, K. Tanaka, H. Hirano, B.E. Nieuwenhuys, ACS Symp. Ser. 552 (1994) 114, (review).
[2] B.E. Nieuwenhuys, Surf. Rev. Lett. 5–6 (1996) 1869, (review).
[3] B.E. Nieuwenhuys, Adv. Catal. 44 (1999) 259, (review).
[4] N.M.H. Janssen, P.D. Cobden, B.E. Nieuwenhuys, J. Phys.: Condens. Matter 9 (1997) 1889, (review) and refs. therein.
[5] R. Imbihl, G. Ertl, Chem. Rev. 95 (1995) 697.
[6] G. Ertl, H.H. Rotermund, Curr. Opin. Solid State Mater. Sci. 1 (1996) 617.
[7] V.P. Zhdanov, B. Kasemo, Surf. Sci. Rep. 20 (1994) 111.
[8] M.F.H. van Tol, P.T. Wouda, B.E. Nieuwenhuys, J. Vac. Sci. Technol. A 12 (1994) 2176.
[9] A.R. Cholach, M.F.H. van Tol, B.E. Nieuwenhuys, Surf. Sci. 320 (1994) 281.
[10] P.D. Cobden, N.M.H. Janssen, Y. van Breugel, B.E. Nieuwenhuys, Faraday Discuss. 105 (1996) 57.
[11] P.D. Cobden, Y. van Breugel, B.E. Nieuwenhuys, Surf. Sci. 402–404 (1998) 155.
[12] F. Mertens, R. Imbihl, Surf. Sci. 347 (1996) 355.
[13] N.M.H. Janssen, A. Schaak, B.E. Nieuwenhuys, R. Imbihl, Surf. Sci. 364 (1996) L555.
[14] P.D. Cobden, J. Siera, B.E. Nieuwenhuys, J. Vac. Sci. Technol. A 10 (1992) 2487.
[15] S. Heinze, V. Schmatloch, N. Kruse, Surf. Sci. 341 (1995) 124.
[16] C.A. de Wolf, B.E. Nieuwenhuys, A. Sasahara, K. Tanaka, M.M. Slinko, M.Yu. Smirnov, Surf. Sci. 411 (1998) L904.
[17] C.A. de Wolf, B.E. Nieuwenhuys, M.M. Slinko, M.Yu. Smirnov, Surf. Sci. 433–435 (1999) 63.
[18] G. Comelli, V.R. Ohanak, M. Kiskinova, K.C. Prince, R. Rossei, Surf. Sci. Rep. 32 (1998) 165.
[19] A.G. Makeev, N.M.H. Janssen, P.D. Cobden, M.M. Slinko, B.E. Nieuwenhuys, J. Chem. Phys. 107 (1997) 965.
[20] C.A. de Wolf, M.O. Hattink, B.E. Nieuwenhuys, accepted for publication in J. Phys. Chem. A Special Somorjai edition.
[21] A. Hornung, M. Muhler, G. Ertl, Catal. Lett. 53 (1998) 77.
[22] P.D. Cobden, B.E. Nieuwenhuys, F. Esch, A. Baraldi, G. Comelli, S. Lizzit, M. Kiskinova, Surf. Sci. 416 (1998) 264.
[23] P.D. Cobden, B.E. Nieuwenhuys, F. Esch, A. Baraldi, G. Comelli, S. Lizzit, M. Kiskinova, J. Vac. Sci. Technol. A 16 (1998) 1014.
[24] F. Esch, A. Baraldi, G. Comelli, S. Lizzit, M. Kiskinova,

P.D. Cobden, B.E. Nieuwenhuys, J. Chem. Phys. 110 (1999) 4013.

[25] C.A. de Wolf, B.E. Nieuwenhuys, A. Baraldi, S. Lizzit, M. Kiskinova, in preparation.

[26] A.V. Walker, M. Gruyters, D.A. King, Surf. Sci. 384 (1997) L791.

[27] M. Gruyters, A.T. Pasteur, D.A. King, J. Chem. Soc., Faraday Trans. 92 (1996) 2941.

[28] A.G. Makeev, B.E. Nieuwenhuys, J. Chem. Phys. 108 (1998) 3740.

[29] A.G. Makeev, B.E. Nieuwenhuys, Surf. Sci. 418 (1998) 432.

[30] F. Schüth, B.E. Henry, L.D. Schmidt, Adv. Catal. 39 (1993) 51.

[31] P. Gardner, R. Martin, R. Nalezinski, C.L.A. Lamont, M.J. Weaver, A.M. Bradshaw, J. Chem. Soc., Faraday Trans. 91 (1995) 3575.

[32] C. Voss, N. Kruse, Appl. Surf. Sci. 87–88 (1994) 134.

[33] M.F.H. van Tol, J. Siera, P.D. Cobden, B.E. Nieuwenhuys, Surf. Sci. 274 (1992) 63.

[34] D.E. Ibbotson, T.S. Wittrig, W.H. Weinberg, Surf. Sci. 111 (1981) 149.

[35] A.G. Makeev, C.A. de Wolf, B.E. Nieuwenhuys, to be published.

[36] A.G. Makeev, M.M. Slinko, N.M.H. Janssen, P.D. Cobden, B.E. Nieuwenhuys, J. Chem. Phys. 105 (1996) 7710.